THE JOURNAL OF BIOLOGICAL CHEMISTRY VOL. 284, NO. 23, pp. 15847–15858, June 5, 2009

Ligand-specific Conformational Changes in the α1 Glycine Receptor Ligand-binding Domain*

Received for publication, December 12, 2008, and in revised form, March 11, 2009 Published, JBC Papers in Press, March 13, 2009, DOI 10.1074/jbc.M809343200

Stephan A. Pless[1] **and Joseph W. Lynch**[2]

From the Queensland Brain Institute and School of Biomedical Sciences, The University of Queensland, Brisbane, Queensland 4072, Australia

Understanding the activation mechanism of Cys loop ion channel receptors is key to understanding their physiological and pharmacological properties under normal and pathological conditions. The ligand-binding domains of these receptors comprise inner and outer β-sheets and structural studies indicate that channel opening is accompanied by conformational rearrangements in both β-sheets. In an attempt to resolve ligand-dependent movements in the ligand-binding domain, we employed voltage-clamp fluorometry on α1 glycine receptors to compare changes mediated by the agonist, glycine, and by the antagonist, strychnine. Voltage-clamp fluorometry involves labeling introduced cysteines with environmentally sensitive fluorophores and inferring structural rearrangements from ligand-induced fluorescence changes. In the inner β-sheet, we labeled residues in loop 2 and in binding domain loops D and E. At each position, strychnine and glycine induced distinct maximal fluorescence responses. The pre-M1 domain responded similarly; at each of four labeled positions glycine produced a strong fluorescence signal, whereas strychnine did not. This suggests that glycine induces conformational changes in the inner β-sheet and pre-M1 domain that may be important for activation, desensitization, or both. In contrast, most labeled residues in loops C and F yielded fluorescence changes identical in magnitude for glycine and strychnine. A notable exception was H201C in loop C. This labeled residue responded differently to glycine and strychnine, thus underlining the importance of loop C in ligand discrimination. These results provide an important step toward mapping the domains crucial for ligand discrimination in the ligand-binding domain of glycine receptors and possibly other Cys loop receptors.

Glycine receptor (GlyR)[3] chloride channels are pentameric Cys loop receptors that mediate fast synaptic transmission in the nervous system (1, 2). This family also includes nicotinic acetylcholine receptors (nAChRs), γ-aminobutyric acid type A and type C receptors, and serotonin type 3 receptors. Individual subunits comprise a large ligand-binding domain (LBD) and a transmembrane domain consisting of four α-helices (M1–M4). The LBD consists of a 10-strand β-sandwich made of an inner β-sheet with six strands and an outer β-sheet with four strands (3). The ligand-binding site is situated at the interface of adjacent subunits and is formed by loops A–C from one subunit and loops D–F from the neighboring subunit (3).

The activation mechanism of Cys loop receptors is currently the subject of intense investigation because it is key to understanding receptor function under normal and pathological conditions (4, 5). Based on structural analysis of *Torpedo* nAChRs, Unwin and colleagues (6, 7) originally proposed that agonist binding induced the inner β-sheet to rotate, whereas the outer β-sheet tilted slightly upwards with loop C clasping around the agonist. These movements were thought to be transmitted to the transmembrane domain via a differential movement of loop 2 (β1-β2) and loop 7 (β6-β7) (both part of the inner β-sheet) and the pre-M1 domain (which is linked via a β-strand to the loop C in the outer sheet). The idea of large loop C movements accompanying agonist binding is supported by structural and functional data (3, 8–13). However, a direct link between loop C movements and channel gating has proved more difficult to establish. Although computational modeling studies have suggested that this loop may be a major component of the channel opening mechanism (14–18), experimental support for this model is not definitive. Similarly, loop F is also thought to move upon ligand binding, although there is as yet no consensus as to whether these changes represent local or global conformational changes (11, 19–21). Recently, a comparison of crystal structures of bacterial Cys loop receptors in the closed and open states revealed that although both the inner and outer β-sheets exhibit different conformations in closed and open states, the pre-M1 domain remains virtually stationary (22, 23). It is therefore relevant to question whether loop C, loop F, and pre-M1 movements are essential for Cys loop receptor activation.

Strychnine is a classical competitive antagonist of GlyRs (24, 25), and to date there is no evidence that it can produce LBD structural changes. In this study we use voltage-clamp fluorometry (VCF) to compare glycine- and strychnine-induced conformational changes in the GlyR loops 2, C, D, E, and F and the pre-M1 domain in an attempt to determine whether they signal ligand-binding events, local conformational changes, or conformational changes associated with receptor activation.

In a typical VCF experiment, a domain of interest is labeled with an environmentally sensitive fluorophore, and current and fluorescence are monitored simultaneously during ligand application. VCF is ideally suited for identifying ligand-specific

* This work was supported by the Australian Research Council and the National Health and Medical Research Council of Australia.

[1] Supported by an International Postgraduate Research Scholarship from the University of Queensland.

[2] Supported by a National Health and Medical Research Council of Australia Senior Research Fellowship. To whom correspondence should be addressed. Tel.: 617-3346-6375; Fax: 617-3346-6301; E-mail: j.lynch@uq.edu.au.

[3] The abbreviations used are: GlyR, glycine receptor; AChBP, acetylcholine-binding protein; AF546, Alexa Fluor 546; LBD, ligand-binding domain; MTSR, methanethiosulfonate-rhodamine; MTS-TAMRA, 2-((5(6)-tetramethylrhodamine) carboxylamino)ethyl methanethiosulfonate; M1–M4, transmembrane segments 1–4; nAChR, nicotinic acetylcholine receptor; TMRM, tetramethylrhodamine-maleimide; VCF, voltage-clamp fluorometry.

conformational changes because it can report on electrophysiologically silent conformational changes (26), such as those induced by antagonists. Indeed, VCF has recently provided valuable insights into the conformational rearrangements of various Cys loop receptors (19, 21, 27–33).

EXPERIMENTAL PROCEDURES

Chemicals—Glycine (Ajax Finechem, Seven Hills, Australia) was dissolved in water and stored at 4 °C. Strychnine (Sigma-Aldrich) was dissolved in Me_2SO (Sigma-Aldrich) and stored at −20 °C. Sulforhodamine methanethiosulfonate (MTSR) and 2-((5(6)-tetramethylrhodamine) carboxylamino)ethyl methanethiosulfonate (MTS-TAMRA) were purchased from Toronto Research Chemicals (North York, Canada). Alexa Fluor 546 C_5 maleimide (AF546) and tetramethylrhodamine-6-maleimide (TMRM) were purchased from Invitrogen. MTSR, MTS-TAMRA, and TMRM were dissolved in Me_2SO and stored at −20 °C. AF546 was dissolved in water on the day of the experiment and stored on ice for up to 6 h.

Molecular Biology—Human GlyR α1 cDNA was subcloned into the pGEMHE vector. All of the constructs generated in this study were made on the α1 GlyR C41A background to eliminate the only uncross-linked extracellular cysteine. QuikChange (Stratagene, La Jolla, CA) was used to generate all of the cysteine mutants used in this study. Automated sequencing of the entire coding sequence confirmed successful incorporation of the mutations. Capped mRNA for oocyte injection was generated using mMessage mMachine (Ambion, Austin, TX).

Oocyte Preparation, Injection, and Labeling—Oocytes from female *Xenopus laevis* (*Xenopus* Express, France) were prepared as previously described (31) and injected with 10 ng of mRNA. The oocytes were then incubated at 18 °C for 3–10 days in an incubation solution containing 96 mM NaCl, 2 mM KCl, 1 mM $MgCl_2$, 1.8 mM $CaCl_2$, 5 mM HEPES, 0.6 mM theophylline, 2.5 mM pyruvic acid, 50 μg/ml gentamycin (Cambrex Corporation, East Rutherford, NJ), pH 7.4.

Fluorophore Labeling—On the day of recording, the oocytes were transferred into ND96 (96 mM NaCl, 2 mM KCl, 1 mM $MgCl_2$, 1.8 mM $CaCl_2$, 5 mM HEPES, pH 7.4) containing 10–20 μM of the dye. Typical labeling times were 30 s for MTSR and MTS-TAMRA (on ice), 30 min for TMRM (on ice), or 45 min for AF546 (at room temperature). The oocytes were then thoroughly washed and stored in ND96 for up to 6 h on ice before recording. All four sulfhydryl-reactive fluorophores employed in this study respond with an increase in quantum efficiency as the hydrophobicity of their environment is increased (27, 28, 30, 34). Each cysteine mutant was incubated with all four fluorophores in turn, and the one yielding the largest fluorescence change (ΔF) upon agonist application was analyzed. Fig. 1 shows a model of the GlyR LBD showing the positions of successfully labeled residues. Because wild type GlyRs never exhibited a ΔF or a change in electrophysiological properties following fluorophore incubation (see Table 1), we can rule out nonspecific effects of the labels.

VCF and Data Analysis—The experimental set up has recently been described in detail (31). In brief, an inverted fluorescence microscope was equipped with a high-Q tetramethylrhodamine isothiocyanate filter set (Chroma Technology, Rockingham, VT), a Plan Fluor 40× objective lens (Nikon Instruments, Kawasaki, Japan), and a PhotoMax 200 photodiode (Dagan Corporation, Minneapolis, MN) with a xenon lamp as light source (Sutter Instruments, Novato, CA). The recording chamber is described in detail in Ref. 28. The cells were voltage-clamped at −40 mV, and currents were recorded with a Gene Clamp 500B amplifier (Axon Instruments, Union City, CA). Current and fluorescence traces were acquired at 200 Hz via a Digidata 1322A interface using Clampex 9.2 software (Axon Instruments). Fluorescence signals were digitally filtered at 1–2 Hz with an eight-pole Bessel filter for analysis and display. Half-maximal concentrations (EC_{50}) and Hill coefficient (n_H) values for ligand-induced activation of current and fluorescence were obtained using the Hill equation fitted with a nonlinear least squares algorithm (SigmaPlot 9.0, Systat Software, Point Richmond, CA). All of the results are expressed as the means ± S.E. of three or more independent experiments.

Spectral Analysis—The spectral analysis methodology has previously been explained in detail (31). In brief, the photodiode was replaced by a MicroSpec 2150i spectrometer (Acton Research Corporation, Acton, MA) coupled to an ORCA-ER CCD camera (Hamamatsu, Hamamatsu City, Japan) and operated using SpectraPro Monochromator Software (Acton Research Corporation, Acton, MA). For excitation, a HQ535/50× filter was used in combination with a Q565LP dichroic mirror (Chroma Technology, Rockingham, VT) and no emission filter. The region of interest was aligned with the slit of the spectrometer and reflected onto the grating (300 g/mm; 500-nm blaze). The extracted spectrum was imaged on the ORCA-ER CCD using MetaMorph 6.2 (Universal Imaging Corporation, Downington, PA). The *x* axis of the resulting "spectral image" represents the wavelength dimension, whereas the *y* axis represents the one-dimensional spatial dimension of the slit. The results from six oocytes were averaged and not subjected to further filtering.

RESULTS

Loop E—The loop E domain in the inner β-sheet forms a β-strand that lines the agonist-binding site (3). VCF studies showed that loop E residues of $GABA_A$ receptor subunits report structural rearrangements that are correlated with channel activation (27, 30). The corresponding GlyR mutants, L127C and R122C, were both investigated in the present study. The location of L127C is indicated in Fig. 1. The L127C mutation resulted in a large decrease in glycine sensitivity that decreased further following labeling with MTS-TAMRA (Table 1). The MTS-TAMRA-labeled L127C mutant GlyR responded with large (~50%) ΔF increases during glycine-mediated activation (Fig. 2*A*). As previously suggested (30, 35), this increased fluorescence is consistent with the idea of a ligand-induced closure of the agonist-binding site. Consistent with both previous studies (27, 30), we found the glycine sensitivity of the change in current (ΔI) and ΔF responses to be identical (Fig. 2, *A* and *B*, and Table 1). Note that the deactivation kinetics often appeared different for ΔF and ΔI signals from the same oocyte (Fig. 2*A*). Because current was recorded from the entire oocyte, whereas fluorescence recorded from a small membrane portion, these

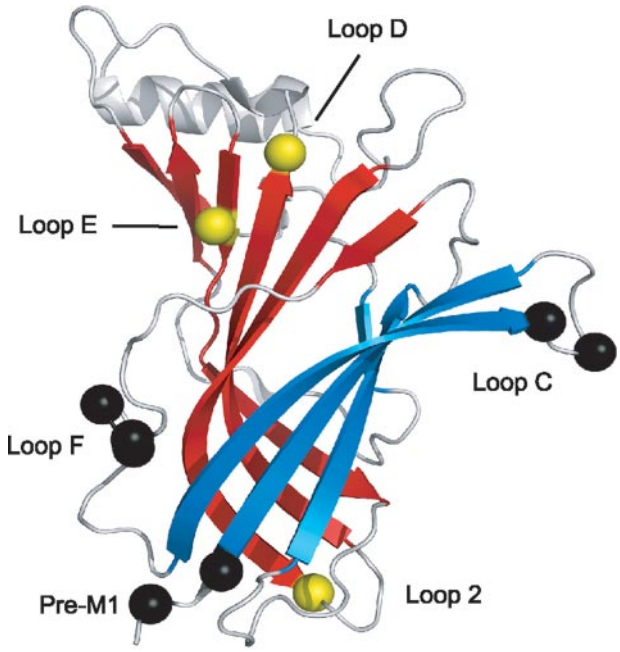

FIGURE 1. **Model of the LBD, based on AChBP bound to carbomylcholine (Protein Data Bank code 1uv6, model generated with PyMOL 0. 99, DeLano Scientific LLC, Palo Alto, CA).** The inner β-sheet is shown in *red*, the outer β-sheet is in *blue*, and the connecting loops are displayed in *gray*. The *black balls* represent approximate locations of residues labeled in loops flanking the outer β-sheet (V178C, A179C, and G181C in loop F; H201C and N203C in loop C; and E217C and Q219C in the pre-M1 domain). G221C and M227C are not shown because they are not present in the AChBP structure. The *yellow balls* show approximate location of residues labeled in the inner β-sheet (L127C in loop E, Q67C in loop D, and A52C in loop 2).

TABLE 1

Summary of results for glycine-evoked current and fluorescence recordings

Displayed are the values for half-maximal activation (EC_{50}), Hill coefficient (n_H), number of experiments (n), and maximal current and fluorescence responses (I_{max} and ΔF_{max}, respectively). All of the results for fluorescence are shown in bold type.

Construct	EC_{50}	n_H	I or ΔF_{max}	n
	μM		μA or %	
WT				
WT ΔI unlabeled	15.5 ± 0.3	2.6 ± 0.1	8.3 ± 0.4	3
WT ΔI MTS-TAMRA	15.6 ± 0.4	2.7 ± 0.1	7.9 ± 0.2	3
WT ΔI TMRM	15.9 ± 0.4	2.7 ± 0.1	6.6 ± 0.5	3
WT ΔI AF546	16.3 ± 0.3	2.5 ± 0.1	6.8 ± 0.9	3
Loop E				
L127C ΔI unlabeled	1020 ± 20	2.4 ± 0.2	7.3 ± 0.3	3
L127C ΔI MTS-TAMRA	4950 ± 180[a]	2.4 ± 0.2	7.7 ± 0.8	7
L127C ΔF MTS-TAMRA	**6070 ± 240[b]**	**1.8 ± 0.1[b]**	**46.7 ± 7.1**	**7**
Loop D				
Q67C ΔI unlabeled	44.1 ± 1.2	2.7 ± 0.1	7.2 ± 0.3	3
Q67C ΔI MTS-TAMRA	63.1 ± 0.6[a]	2.9 ± 0.1	7.2 ± 0.5	3
Q67C ΔF MTS-TAMRA	**1180 ± 50[b]**	**1.7 ± 0.1[b]**	**18.0 ± 0.6**	**3**
Loop F				
V178C ΔI unlabeled	47.4 ± 1.0	2.6 ± 0.1	12.3 ± 1.8	5
V178C ΔI AF546	40.7 ± 0.1	2.6 ± 0.1	10.3 ± 2.3	8
V178C ΔF AF546	**313 ± 20[b]**	**1.3 ± 0.1[b]**	**12.6 ± 0.6**	**9**
A17C ΔI unlabeled	83.6 ± 5.0	2.6 ± 0.5	8.0 ± 0.6	4
A179C ΔI MTS-TAMRA	135 ± 9[a]	1.7 ± 0.2[a]	8.4 ± 0.3	4
A179C ΔF MTS-TAMRA	**642 ± 117[b]**	**1.5 ± 0.4**	**2.2 ± 0.6**	**3**
G181C unlabeled	29.3 ± 0.8	2.8 ± 0.3	7.6 ± 0.4	5
G181C MTSR	39.8 ± 1.3	1.9 ± 0.1[a]	9.9 ± 2.1	5
G181C ΔF MTSR	**503 ± 65[b]**	**1.3 ± 0.2[b]**	**11.6 ± 2.7**	**6**
Loop C				
H201C ΔI unlabeled	17.9 ± 0.6	2.9 ± 0.2	10.3 ± 1.0	5
H201C ΔI MTS-TAMRA	16.3 ± 0.6	2.9 ± 0.2	9.3 ± 0.8	6
H201C ΔF MTS-TAMRA	**126 ± 3[b]**	**2.1 ± 0.1[b]**	**10.2 ± 1.0**	**5**
N203C ΔI unlabeled	25.9 ± 0.2	3.0 ± 0.1	6.6 ± 0.5	3
N203C ΔI MTS-TAMRA	45.7 ± 1.2[a]	3.0 ± 0.2	6.9 ± 0.2	6
N203C ΔF MTS-TAMRA	**526 ± 25[b]**	**1.2 ± 0.1[b]**	**44.3 ± 5.9**	**6**
Loop 2				
A52C ΔI unlabeled	18.5 ± 0.1	3.2 ± 0.1	7.8 ± 0.2	3
A52C ΔI MTS-TAMRA	17.4 ± 0.1	3.0 ± 0.1	7.7 ± 0.2	4
A52C ΔF MTS-TAMRA	**201 ± 10[b]**	**1.4 ± 0.1[b]**	**−8.6 ± 1.1**	**4**
Pre-M1				
E217C ΔI unlabeled	30.2 ± 0.1	2.6 ± 0.4	17.6 ± 3.6	4
E217C ΔI TMRM	27.1 ± 0.1	3.2 ± 0.4	17.0 ± 0.6	3
E217C ΔF TMRM	**135 ± 9.4[b]**	**1.9 ± 0.2[b]**	**−1.8 ± 0.5**	**3**
Q219C ΔI unlabeled	20.9 ± 0.9	2.6 ± 0.2	8.3 ± 0.4	8
Q219C ΔI MTSR	9.2 ± 0.2[a]	2.6 ± 0.2	8.4 ± 0.4	7
Q219C ΔF MTSR	**98.6 ± 9.9[b]**	**1.5 ± 0.2[b]**	**−13.3 ± 0.8**	**9**
G221C ΔI unlabeled	5.6 ± 0.4	2.3 ± 0.2	5.5 ± 0.1	3
G221C ΔI MTS-TAMRA	2.0 ± 0.2[a]	1.8 ± 0.3	2.9 ± 0.3[a]	4
G221C ΔF MTS-TAMRA	**6.8 ± 0.1[b]**	**1.8 ± 0.1**	**−16.3 ± 0.9**	**4**
M227C ΔI unlabeled	28.7 ± 0.1	2.9 ± 0.1	7.8 ± 0.8	3
M227C ΔI AF546	13.1 ± 0.1[a]	2.4 ± 0.1[a]	6.5 ± 0.5	3
M227C ΔF AF546	**226 ± 24[b]**	**1.0 ± 0.1[b]**	**−3.5 ± 0.3**	**3**

[a] Significant difference to electrophysiological properties of unlabeled oocytes (Student's t test; $p < 0.05$).
[b] Significant difference of fluorescence properties to electrophysiological properties after labeling (Student's t test; $p < 0.05$).

effects may have been due to nonuniform solution exchange profiles around the oocyte.

Application of the competitive antagonist strychnine in the absence of glycine also evoked large ΔF signals (Fig. 2*C*). These signals exhibited a mean EC_{50} of 280 ± 22 nM, an n_H of 1.1 ± 0.1, and a ΔF_{max} of 147 ± 43% ($n = 5$ cells). Because the strychnine ΔF_{max} was three times greater than that produced by a saturating glycine concentration (Fig. 2*D*), it is likely that the two compounds induced distinct structural changes. To further test this possibility, we performed a spectroscopic analysis of the fluorescence signal before, during, and after the application of glycine or strychnine (Fig. 2*E*). We found that glycine application increased the quantum yield but did not significantly shift the emission peak (compared with the emission peak before glycine application). However, strychnine application produced both an increase in quantum yield and a ~4-nm blue shift in the emission spectrum (Fig. 2*F*). This highly significant difference ($p < 0.001$) suggests that glycine-induced conformational changes are mainly evoked by dequenching, whereas strychnine-induced movements also result in an increased hydrophobicity in the fluorophore environment. This finding supports the idea of ligand-specific conformational changes at L127C.

Labeling with MTSR produced similar results to MTS-TAMRA, although AF546 and TMRM produced no significant glycine-dependent ΔF (n = 3–5 cells each). Although the AF546-labeled E122C in the $GABA_A$ receptor β_2 subunit produces ΔF responses that correlate well with channel activation (30), the corresponding GlyR mutant (R122C) did not give rise to a significant ΔF with any of the four fluorophores.

Loop D—Like loop E, loop D is a β-strand on the inner β-sheet. A portion of this strand contributes to the complementary (−) side of the GlyR-binding pocket (36). Because Phe^{63} and Arg^{65} in loop D are important residues for ligand binding (36, 37), we reasoned that the adjacent residues on the same side of the β-strand, Q67C and N69C, may report on conformational rearrangements during agonist and antagonist binding. Introduction of the Q67C mutation led to a minor increase in the current EC_{50}, which increased further after incubation with MTS-TAMRA (Table 1). Glycine application to Q67C-injected oocytes labeled with MTS-TAMRA evoked

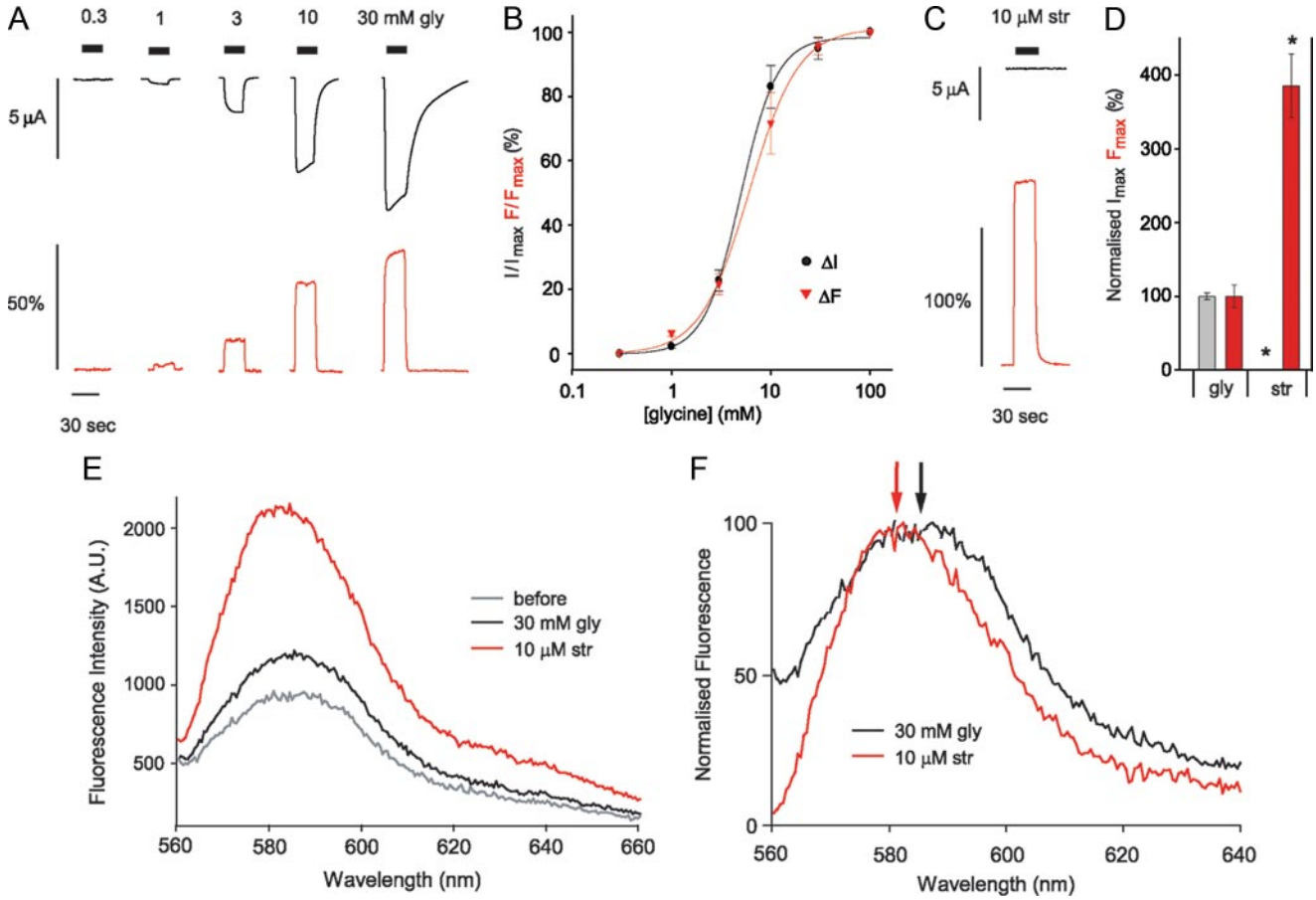

FIGURE 2. **Glycine and strychnine induce distinct conformations around L127C in loop E.** *A*, glycine-induced current (*black*) and fluorescence (*red*) traces recorded from oocytes injected with L127C. *B*, averaged dose-response relationships for glycine. *C*, strychnine-induced current (*black*) and fluorescence (*red*) responses at a saturating strychnine concentration. In this and subsequent figures, the *horizontal bars* denote the duration of glycine (*gly*) or strychnine (*str*) application. *D*, comparison of maximal current (*gray*) and maximal fluorescence (*red*) responses for glycine and strychnine. The data normalized to mean glycine values. *, $p < 0.0005$. *E*, spectral emission from MTSR-labeled L127C oocytes before (*gray*) and during the application of glycine (*black*) or strychnine (*red*) (average of six cells each). Note that the trace obtained after the application of both ligands is omitted for clarity, because it was identical to the trace before the application of ligands (*gray*). *F*, normalized difference emission spectra recorded during application of glycine and strychnine. The spectra recorded in the absence of glycine were subtracted from spectra recorded in the presence of glycine (*black*) and strychnine (*red*), respectively (the *traces* were normalized to the strychnine response; average of six cells each). The *arrows* indicate the emission peak of glycine (*black*) and strychnine (*red*). Glycine showed no significant shift in the emission peak compared with the emission peak before ligand application ($\Delta\lambda = 0.1 \pm 0.2$ nm, $n = 6$). However, the emission peak during strychnine application was significantly ($p < 0.001$) blue -shifted compared with the emission peak before ligand application ($\Delta\lambda = 3.8 \pm 0.4$ nm, $n = 6$).

large (~ 20%) fluorescence changes (Fig. 3*A*). The current EC_{50} was significantly lower than the fluorescence EC_{50}, whereas n_H showed the opposite trend (Fig. 3*B*). Application of strychnine led to dramatically larger ΔF values than those induced by glycine ($F_{max} = 213 \pm 80\%$, EC_{50} 1.4 ± 0.1 μM, $n_H = 1.5 \pm 0.1$, $n = 4$) (Fig. 3, *C* and *D*), suggesting distinct conformations. Attempts to label the adjacent N69C residue were unsuccessful; we observed robust currents but no change in glycine sensitivity or a ΔF after incubation with any of the four dyes ($n = 3–4$ each).

Loop F—Loop F is an unstructured region located at the bottom of the agonist-binding site (Fig. 1) (3, 11). A number of studies have proposed this loop as an important element of the Cys loop receptor gating mechanism (21, 38–40), although one VCF study has recently challenged this view (19). To determine whether conformational rearrangements in GlyR loop F discriminate between agonists and antagonists, we investigated four consecutive mutants in this region: V178C, A179C, D180C, and G181C. The V178C mutation produced a significant but small increase in the glycine ΔI EC_{50} (Table 1) that did not change following incubation with any of the four fluorophores. After incubation with AF546, oocytes injected with the V178C mutant GlyR produced ΔF_{max} signals of ~10% (Fig. 4*A* and Table 1). The glycine ΔI EC_{50} was significantly lower than that of ΔF, with n_H showing the opposite trend (Fig. 4, *A* and *B*, and Table 1). As expected, the competitive antagonist strychnine did not produce a ΔI but elicited a concentration-dependent ΔF of the same sign as glycine (Fig. 4*C*). Averaged from seven oocytes, the strychnine concentration-response curve was fitted by an EC_{50} of 127 ± 9 nM, an n_H of 1.6 ± 0.2, and a ΔF_{max} of 10.0 ± 1.6%. Importantly, the ΔF_{max} values were virtually identical for glycine and strychnine (Fig. 4*D*), suggesting a similar structural rearrangement.

The A179C mutant GlyR exhibited a moderate (~5-fold) decrease in glycine sensitivity (Table 1). Labeling with MTS-TAMRA further decreased the glycine sensitivity and gave rise to small (~2%) ΔF_{max} signals. Again, the ΔI EC_{50} was significantly lower than the ΔF EC_{50}, with the n_H showing the opposite trend (Table 1). No ΔF was observed following incubation of the adjacent D180C mutation with any of the fluorophores,

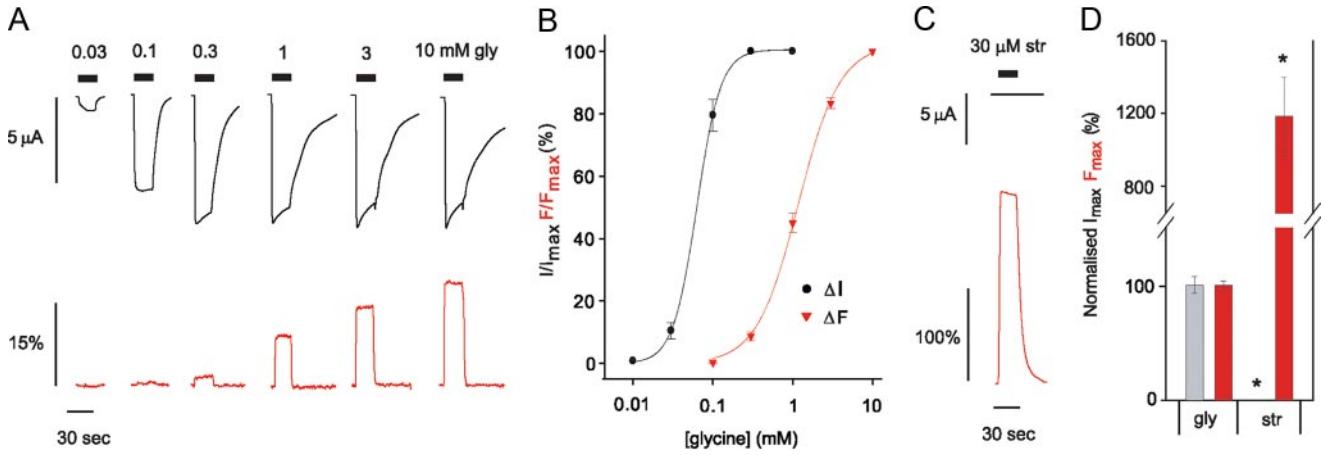

FIGURE 3. **Glycine and strychnine induce distinct conformations around Q67C in loop D.** *A*, glycine-induced current (*black*) and fluorescence (*red*) traces recorded from oocytes injected with Q67C. *B*, averaged dose-response relationships for glycine (*gly*). *C*, strychnine-induced current (*black*) and fluorescence (*red*) responses at a saturating strychnine (*str*) concentration. *D*, comparison of maximal current (*gray*) and maximal fluorescence (*red*) responses for glycine and strychnine. Note the broken *y* axis. The data normalized to mean glycine values. *, $p < 0.0005$

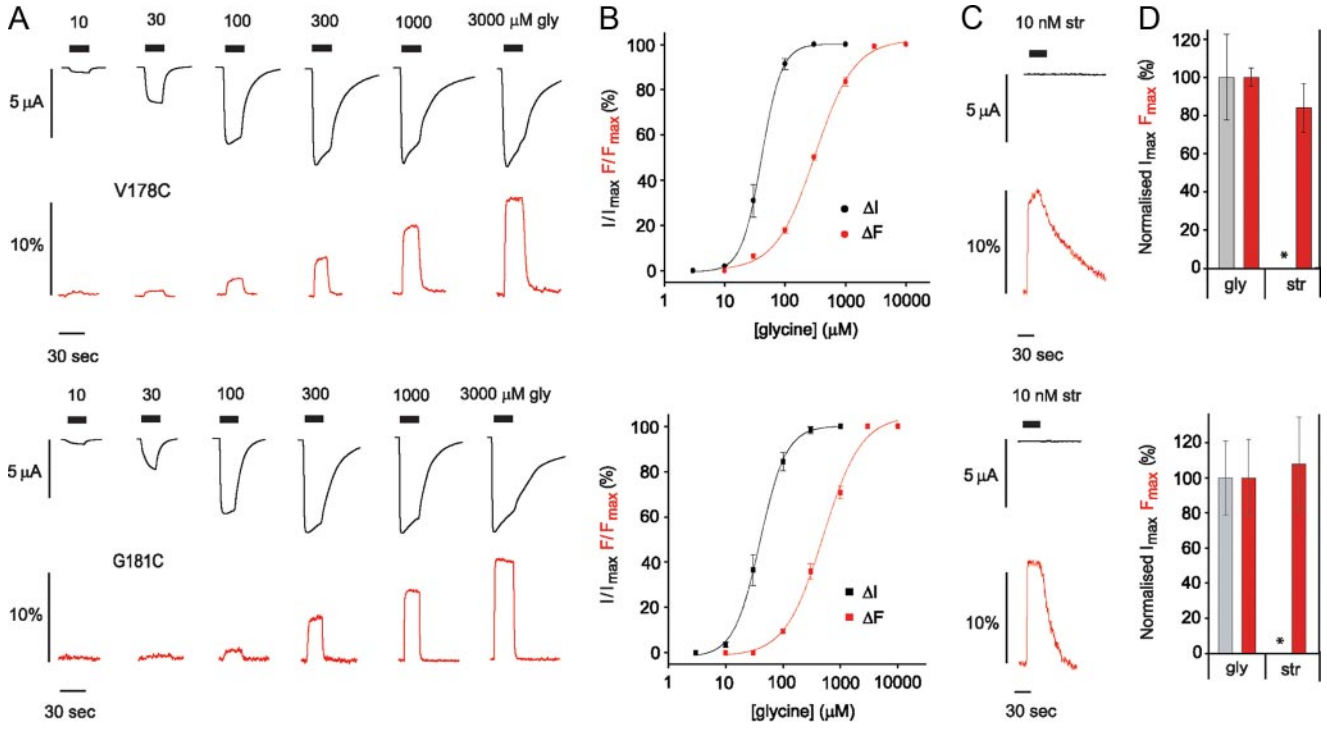

FIGURE 4. **Glycine and strychnine induce similar conformational changes in loop F.** *A*, glycine-induced current (*black*) and fluorescence (*red*) traces recorded from oocytes injected with V178C (*upper panel*) or G181C (*lower panel*). *B*, averaged dose-response relationships for glycine (*gly*). *C*, strychnine-induced current (*black*) and fluorescence (*red*) responses at a saturating strychnine (*str*) concentration. *D*, comparison of maximal current (*gray*) and maximal fluorescence (*red*) responses for V178C (*upper panel*) and G181C (*lower panel*). The data are normalized to the mean glycine values. *, $p < 0.0005$.

although the current EC_{50} was significantly increased after labeling with MTSR (D180C unlabeled: $EC_{50} = 58.6 \pm 2.7$ μM, $n_H = 1.9 \pm 0.1$, $I_{max} = 6.0 \pm 1.3$ μA; after labeling with MTSR: $EC_{50} = 98.8 \pm 0.1$ μM, $n_H = 2.3 \pm 0.5$, $I_{max} = 6.9 \pm 0.1$ μA; $n = 4$ each).

MTSR labeling resulted in large (>10%) ΔF_{max} values at G181C mutant GlyR (Fig. 4*A*). Again, the EC_{50} for ΔI was significantly lower than that for ΔF, whereas the n_H value was significantly lower for ΔF (Fig. 4, *A* and *B*, and Table 1). ΔF_{max} induced by the antagonist strychnine did not vary from those induced by agonists (Fig. 4, *C* and *D*). The mean strychnine ΔF concentration response, averaged from four oocytes, yielded an EC_{50} of 208 ± 25 nM, an n_H of 1.2 ± 0.1, and a ΔF_{max} of 12.6 ± 3.1%.

Loop C—Loop C is a relatively flexible domain that adopts an extended conformation in the absence of agonist (10, 16, 41). Upon agonist binding it is hypothesized to undergo a large motion to cap the ligand-binding site (5, 6, 11, 42). This capping motion has been suggested to serve as a trigger for channel opening (5, 12, 15, 43), although to date there is little direct experimental evidence for this. Importantly, structural studies have suggested that loop C shows ligand-specific movements (8, 9, 11), although a recent VCF study could neither entirely prove or dismiss this hypothesis (27). We avoided investigating

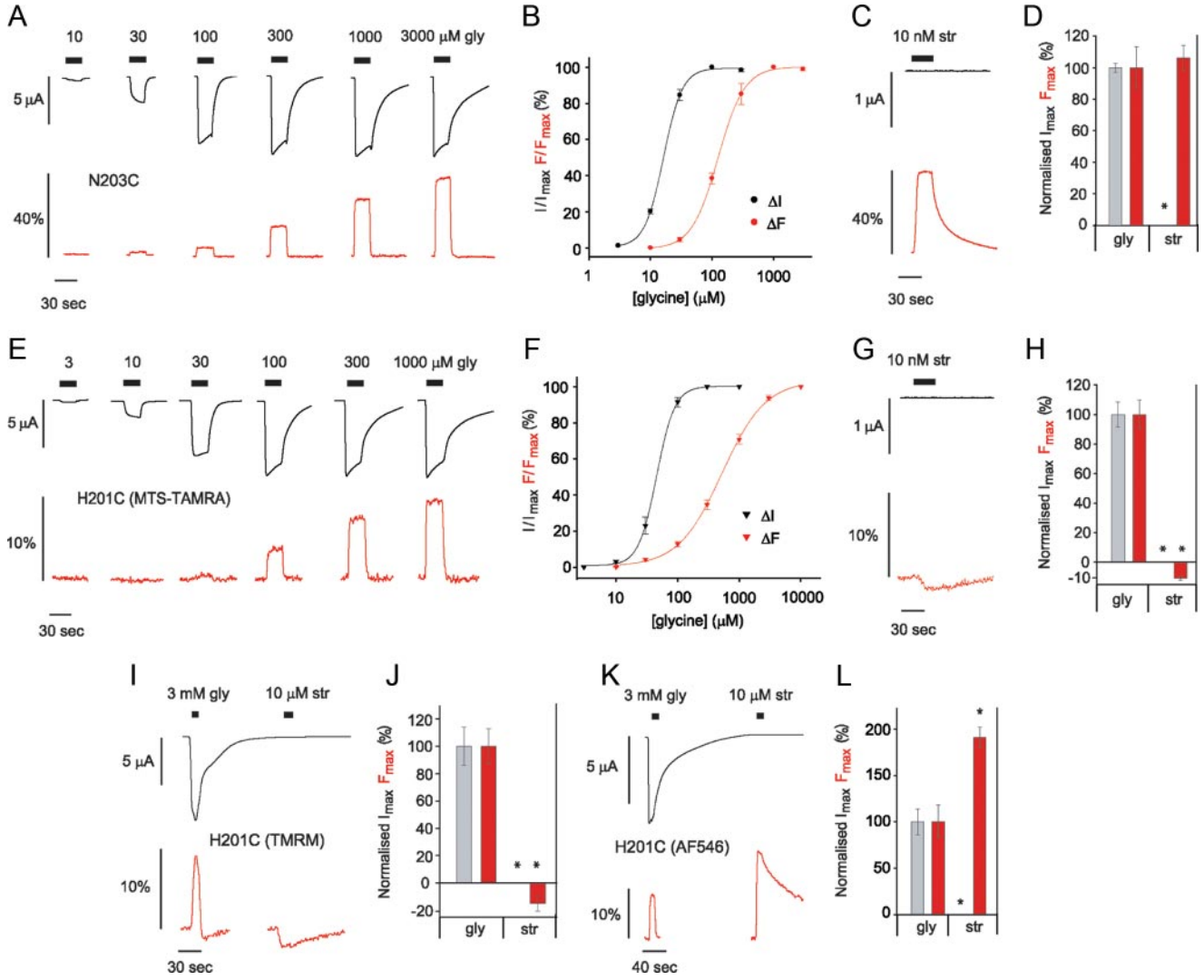

FIGURE 5. **Conformational rearrangements in loop C partially discriminate between glycine and strychnine.** *A*, glycine-induced current (*black*) and fluorescence (*red*) traces recorded from oocytes injected with N203C. *B*, averaged dose-response relationships for glycine (*gly*). *C*, strychnine-induced current (*black*) and fluorescence (*red*) responses at a saturating strychnine (*str*) concentration. *D*, comparison of maximal current (*gray*) and maximal fluorescence (*red*) responses for N203C. *E*, glycine-induced current (*black*) and fluorescence (*red*) traces recorded from oocytes injected with H201C. *F*, averaged dose-response relationships for glycine. *G*, strychnine-induced current (*black*) and fluorescence (*red*) responses at a saturating strychnine concentration. *H*, comparison of maximal current (*gray*) and maximal fluorescence (*red*) responses for H201C. Note the broken *y* axis. *I* and *K*, glycine and strychnine induced current (*black*) and fluorescence (*red*) traces recorded from oocytes injected with H201C labeled with TMRM (*I*) or AF546 (*K*). *J* and *L*, comparison of maximal current (*gray*) and maximal fluorescence (*red*) responses for H201C labeled with TMRM (*J*) or AF546 (*L*). The data are normalized to the mean glycine values. *, $p < 0.05$.

loop C residues Lys^{200}, Tyr^{202}, Thr^{204}, and Phe^{207} because they are important ligand-binding residues (36, 37, 44, 45). Because alanine mutations of the adjacent residues His^{201}, Asn^{203}, and Lys^{206} have modest effects on agonist and antagonist binding (45), we introduced cysteines individually at these positions. Oocytes expressing the N203C mutant GlyR showed a significant decrease in glycine sensitivity and robust ΔF values after labeling with MTS-TAMRA (Table 1 and Fig. 5*A*). As shown in Fig. 5*B* and summarized in Table 1, the glycine ΔI EC_{50} was significantly lower than that for the ΔF signal, and the ΔF n_H was significantly decreased. When applied alone, strychnine also produced large ΔF signals (Fig. 5*C*). The averaged strychnine dose-response yielded a ΔF EC_{50} of 458 ± 13 nM, an n_H of 2.1 ± 0.1, and a ΔF_{max} of 47.0 ± 3.5% (all $n = 4$). Because the ΔF_{max} signals for glycine and strychnine displayed no significant difference in sign or size (Fig. 5*D*), we conclude that the fluorophore attached to N203C reported identical structural rearrangements for glycine and strychnine.

The ΔI EC_{50} for H201C did not change following labeling with MTS-TAMRA (Table 1). Labeling with MTS-TAMRA resulted in large ΔF signals (Fig. 5*E*). The glycine ΔI EC_{50} was significantly lower than that of the ΔF signal, whereas n_H was significantly lower for ΔF (Fig. 5, *E* and *F*, and Table 1). Interestingly, strychnine produced ΔF signals of the opposite sign (Fig. 5, *G* and *H*), although the small size of the signal (ΔF_{max} ~1%, $n = 4$) precluded quantitative analysis. To further examine a possible distinct conformational change, we also labeled H201C with TMRM and subsequently obtained almost identical results (Fig. 5, *I* and *J*). In contrast to MTS-TAMRA and TMRM, labeling H201C with AF546 led to an increased fluorescence in response to both glycine and strychnine (Fig. 5*K*). However, we found the ΔF_{max} for strychnine to be significantly

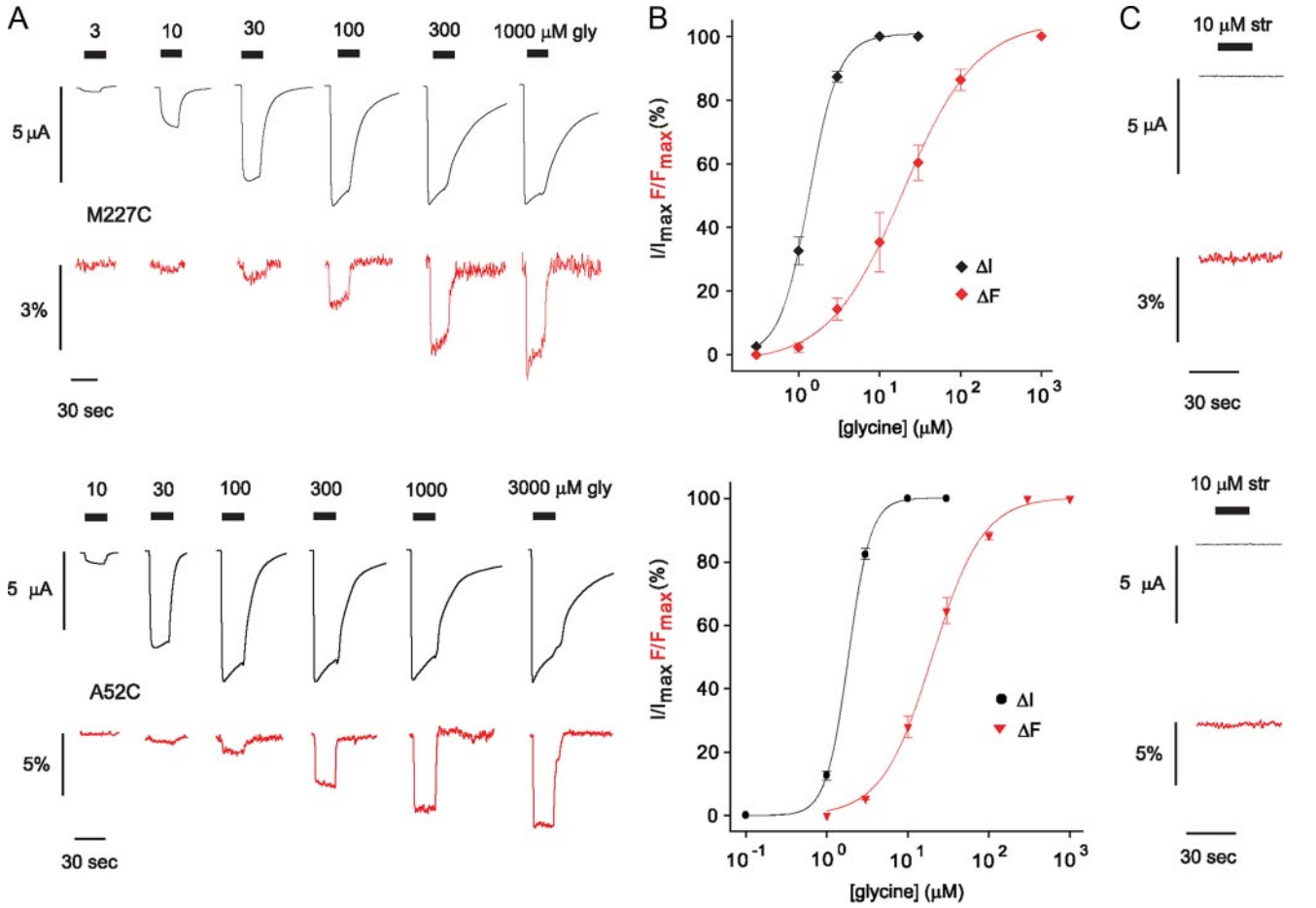

FIGURE 6. **Loop 2 and the pre-M1 domain undergo conformational changes in response to glycine application, but not to strychnine application.** *A*, glycine-induced current (*black*) and fluorescence (*red*) traces recorded from oocytes injected with M227C (*upper panel*) or A52C (*lower panel*). *B*, averaged dose-response relationships for glycine (*gly*). *C*, strychnine-induced current (*black*) and fluorescence (*red*) responses at a high strychnine (*str*) concentration.

($p < 0.05$) larger than that for glycine (ΔF_{max} strychnine = 18.0 ± 1.0% ($n = 3$) *versus* ΔF_{max} glycine = 9.4 ± 1.8% ($n = 3$)) (Fig. 5, *K* and *L*). Taken together, these results strongly suggest ligand-specific structural rearrangements at H201C. Furthermore, they also demonstrate that distinct conformational changes can be displayed by differences in sign or size of the fluorescence signal. K206C did not exhibit a significant glycine ΔI EC_{50} change or a significant ΔF following incubation with any of the fluorophores.

Pre-M1—We mutated all residues from Glu^{217} to Met^{227} to cysteines, with the exception of Arg^{218}, Tyr^{222}, and Tyr^{233} because cysteine mutations at these positions preclude the functional expression of GlyRs.[4] The I220C, L224C, I225C, and Q226C mutations all produced no change in glycine ΔI EC_{50} and no ΔF signal following incubation with any of the four fluorophores. We thus conclude that these residues are not labeled. In contrast, Q219C was successfully labeled with MTSR, as demonstrated by the significantly decreased ΔI EC_{50} after MTSR incubation and the robust glycine-induced decrease in ΔF (Table 1). The ΔI EC_{50} was substantially lower than that of ΔF, whereas n_H was significantly higher (Table 1). Similar results were obtained from E217C, G221C, and M227C mutants labeled with TMRM, MTS-TAMRA, and AF546, respectively (Fig. 6*A* and Table 1). Additionally, n_H was significantly lower for ΔF than for ΔI (Fig. 6*B* and Table 1). Importantly, none of these labeled residues in the pre-M1 domain showed a fluorescence signal in response to application of high (10 μM) strychnine concentrations ($n = 4$ each) (Fig. 6*C*).

Loop 2—Loop 2, which is directly connected to loop D in the inner β-sheet, has previously been implicated in channel gating in GlyRs and nAChRs (5, 46). In an attempt to investigate ligand-induced conformational changes in this domain, we created the following cysteine mutants: A52C, E53C, T54C, T55C, and M56C. The A52C mutation resulted in a receptor with wild type-like electrophysiological properties, and labeling with MTS-TAMRA had no effect on the current EC_{50}. However, it exhibited a robust decrease in fluorescence in response to glycine application (Table 1 and Fig. 6*A*). Again, the ΔI EC_{50} was significantly lower than that of ΔF (Fig. 6*B* and Table 1). Similar to the situation in the pre-M1 domain, even high (10 μM) concentrations of strychnine failed to elicit detectable changes in fluorescence ($n = 4$) (Fig. 6*C*). The E53C and T54C mutants both showed significantly smaller maximal currents (I_{max} = 4.0 ± 0.2 μA, $n = 3$ and I_{max} = 4.1 ± 0.3 μA, $n = 3$), and there was no evidence of labeling with any of the dyes, as indicated by the lack of change in current EC_{50} and lack of ΔF after the

[4] S. T. Nevin and J. W. Lynch, unpublished results.

labeling procedure (data not shown). Because the T55C and M56C mutants generated only very small (<0.5 μA, $n = 3–4$) currents, they were not further analyzed.

DISCUSSION

General Considerations—Several factors must be taken into account when interpreting data from VCF studies. First, the absence of a measurable ΔF does not preclude the possibility of a conformational change taking place. In fact, a fluorophore may move a considerable distance between two distinct states of the receptor, but if the local environment does not change sufficiently, a ΔF will not be observed. Similarly, we make the assumption that identical fluorescence changes report similar changes in hydrophobicity. We acknowledge, however, that an identical change in fluorescence for two ligands could also report a different conformational change, because distinct conformations may expose the fluorophore to similarly hydrophobic environments. Additionally, because of the size of the fluorophore and the length of the linker, it is possible that the ΔF is reporting on a conformational change that occurs at some distance from labeled site, whereas the site itself remains stationary. Where possible, we attempted to overcome these complications by labeling multiple residues in a given domain. We reasoned that if multiple positions in a domain report similar changes, more generalized conclusions could be drawn about the role of that domain. Furthermore, an observed ΔF may report on an electrophysiologically silent conformational change. Finally, as discussed in more detail below, the ΔF can report on more than one conformational change, and it may thus be difficult to separate conformational changes associated with activation from those associated with desensitization. Because of these limitations, we focus on differences (or similarities) in the sign and/or size of the ΔF signals produced by agonists and antagonists.

Desensitization—Because of the slow rate of agonist application when working with ligand-gated ion channels in the *Xenopus* expression system, it may be difficult to discriminate between a ΔF associated with channel activation and a ΔF evoked by another event, such as desensitization. Thus, in principle, an observed ΔF might be due to a transition from a closed to a desensitized or from an open to a desensitized state. In fact, the large number of residues in this study showing a dramatically higher EC_{50} (and lower n_H) for fluorescence than for current may suggest that they detect a conformational change associated with desensitization. Consequently, we will consider the possibility that ΔF signals may reflect desensitized states in the following discussion.

Inner β-Sheet—Because recent structural studies (22, 23) showed that receptor activation is accompanied by rearrangements of the entire inner β-sheet, we sought to detect these movements by fluorescently labeling various positions in the inner β-sheet.

The labeled L127C residue exhibits overlapping glycine ΔF and ΔI concentration-response relations. Furthermore, the magnitude of the ΔF_{max} signals is strongly ligand-dependent, indicating that glycine and strychnine induce distinct structural rearrangements at L127C. This finding is supported by a spectroscopic analysis of the fluorescence signal, which showed a blue shift in the emission spectrum for strychnine but not for glycine. The overlapping ΔI and ΔF dose-response curves suggest that this residue senses a conformational change associated with the open channel state. Thus, both lines of evidence support a role for loop E in activation. Such a conclusion would agree with recent structural data showing large conformational changes in this domain during activation (22, 23). It also agrees well with previous VCF studies. The fluorescence recorded from equivalent or nearby loop E residues in the $GABA_A$ and the $GABA_C$ receptors (27, 30) also displayed overlapping glycine ΔF and ΔI concentration responses, and the ΔF signals were different for agonists and antagonists. A role for loop E in receptor activation is also supported by single channel kinetic analyses in the nAChR (50, 51).

Our results from loop D also suggest distinct structural rearrangements in response to glycine and strychnine. A recent study using site-directed mutagenesis and modeling had suggested distinct conformations for agonist and antagonist binding at the GlyR Arg^{65} residue in loop D (36), but direct experimental evidence was lacking. Here, we report highly ligand-specific conformational changes at the adjacent Gln^{67} position. Additionally, we demonstrate that loop 2 (which is directly connected to loop D and also part of the inner β-sheet) detects a glycine-induced conformational change but seems to remain stationary when strychnine is bound. A number of studies have previously provided evidence for a network of salt bridges connecting the LBD and the M2-M3 linker region via loop 2 (43, 46, 52–55). Given the close physical proximity of loop 2 to the M2-M3 linker of the transmembrane domain, which also moves in response to agonists but not antagonists in both GlyRs and $GABA_A$ receptors (31, 32), the conformational change we detect in loop 2 may reflect an activated or desensitized state. Taken together, these findings emphasize the crucial role of the inner β-sheet in ligand recognition and, more importantly, in ligand discrimination.

Loop F—The labeled loop F residues, V178C and G181C, showed no discrimination between binding of glycine and strychnine. This is a somewhat surprising finding, given the close proximity to the binding site and the substantial size difference between glycine and strychnine. However, it is consistent with earlier observations that the relatively large structural rearrangements in the AChBP loop F occur in response to both agonist and antagonist binding (11) and that the loop F domain of serotonin type 3 receptors (20) undergoes ligand-induced rearrangements that do not necessarily discriminate between agonists and antagonists. Additionally, a recent VCF study on the $GABA_C$ loop F has found identical ΔF responses for both agonists and antagonists at T218C, a residue that corresponds to V178C in the GlyR (21). It is thus conceivable that loop F, as recently suggested by others (19), plays a major role in ligand docking, but not necessarily in receptor activation.

Loop C—Our data suggest that loop C undergoes structural rearrangements in response to ligand binding, in agreement with structural (6, 7, 9, 11, 42) and computational modeling studies (14–18). Interestingly, a VCF study on a the $GABA_C$ loop C also observed conformational changes in response to both agonists and antagonists (27). However, the maximum signal amplitudes could not be determined, making a direct

comparison between agonist and antagonist-induced movements difficult (27).

Similar to the situation in loop F, N203C displayed identical fluorescence changes in response to agonist and antagonist binding. This is an important finding, because a previous AChBP crystallographic study has suggested that loop C globally distinguishes between agonists and antagonists (11). However, consistent with the findings of that study, we found that the labeled H201C GlyR responded differently to glycine and strychnine. For example, TMRM and MTS-TAMRA labels both yielded increases in ΔF upon glycine binding but reductions in ΔF upon strychnine binding. In contrast, AF546 yielded an increased ΔF upon the binding of both strychnine and glycine, although the strychnine ΔF was significantly larger. Moreover, Lys^{200} and Tyr^{202} are among the few residues in the GlyR-binding site whose orientation differs markedly between glycine binding and strychnine binding (36, 44). Hence it is not surprising that fluorophores attached to H201C recognize these ligand-specific movements. The fact that fluorophores attached to the nearby N203C do not respond differently to glycine and strychnine binding is an example for the high spatial resolution of VCF.

Another interesting aspect of our results from loop C is the fluorophore-dependent ΔF in response to strychnine application. A possible explanation for this result is the different linker length between fluorophore and cysteine side chain for the fluorophores used here. Linker lengths are likely to be 5, 7.8, 7.8, and 15.1 Å for TMRM, MTSR, MTS-TAMRA, and AF546, respectively (30). Thus, because the AF546 linker is substantially longer than those of TMRM and MTS-TAMRA, we speculate that it senses a different change in environment upon strychnine binding.

In conclusion, our results emphasize that loop C does discriminate between agonists and antagonists, although not over its entire length. Given the importance of loop C for ligand binding and possibly channel activation in Cys loop receptors, our findings offer insight into the allosteric mechanisms of this crucial domain.

Pre-M1 Domain—Other studies inferred a crucial role for the pre-M1 domain based on state-dependent changes in the strength of electrostatic interactions between oppositely charged residues in the pre-M1 domain and LBD loops $\beta1$-$\beta2$ or $\beta6$-$\beta7$ (43, 56). However, recent crystal structures of bacterial Cys loop receptors suggested only a minimal movement of the pre-M1 domain during transition from closed to open (22, 23). Here, we clearly identified agonist-induced structural rearrangements in the pre-M1 domain. On the other hand, we found no evidence for strychnine-induced conformational changes at any of the four labeled pre-M1 domain residues. Because glycine opens the channel, whereas strychnine does not, it seems reasonable to conclude that the pre-M1 domain senses a conformational change associated with either an activated or desensitized state.

A Direct Ligand-Fluorophore Interaction?—Theoretically, the ligand-mediated ΔF responses observed here could originate from direct quenching or dequenching induced by the binding of ligands near the fluorophore. Based on the following arguments, we consider this scenario unlikely. First, a direct ligand-fluorophore interaction would produce a ΔF at concentrations lower than those required for channel activation, because GlyR require two to three bound glycine molecules to open (47, 48). This was not the case; at L127C current and fluorescence were superimposed at low concentrations, and at all other sites ΔF was significantly right-shifted. Second, in loop F the ΔF_{max} values were identical for structurally very different ligands (*e.g.* glycine and strychnine at V178C and G181C). Third, agonists and antagonists have previously been shown to exert no influence on fluorophores tethered close to the binding sites of other Cys loop receptors (19, 21, 27, 30, 32). Additionally, direct ligand-fluorophore interactions seem particularly unlikely in loop 2 and in the pre-M1 domain, because these domains are physically distant from the ligand-binding site. Taken together, these observations are not compatible with a ligand-induced quench or dequench of any residue investigated here.

Conclusion—In this study we identified through fluorophore labeling 12 residues in the GlyR LBD that sense conformational changes upon ligand binding. More importantly, we demonstrate that eight of these residues show ligand-specific conformational changes, discriminating between the agonist glycine and the competitive antagonist strychnine. Four aspects are particularly noteworthy: 1) the competitive antagonist strychnine induces conformational changes near the binding site only and not at the interface with the transmembrane domain; 2) one residue in loop C discriminates between glycine and strychnine, whereas another does not; these findings indicate that loop C is important for ligand discrimination, although not over its entire length; 3) three residues in the inner β-sheet discriminate between agonists and antagonists, underlining the crucial role of this domain in agonist-specific actions; 4) loop F, although in close physical proximity to the binding site, does not discriminate between agonists and antagonists. Thus, loop F may sense conformational changes that are not essential for activation. Taken together, these results shed new light on the conformational variability of the GlyR LBD and extend our knowledge about the allosteric mechanisms involved in Cys loop receptor function.

Acknowledgment—We thank Dr. Tim Webb for insightful discussions and comments on the manuscript.

REFERENCES

1. Barnard, E. A. (1992) *Trends Biochem. Sci.* **17,** 368–374
2. Le Novere, N., and Changeux, J. P. (2001) *Philos. Trans. R. Soc. Lond. B Biol. Sci.* **356,** 1121–1130
3. Brejc, K., van Dijk, W. J., Klaassen, R. V., Schuurmans, M., van Der Oost, J., Smit, A. B., and Sixma, T. K. (2001) *Nature* **411,** 269–276
4. Lester, H. A., Dibas, M. I., Dahan, D. S., Leite, J. F., and Dougherty, D. A. (2004) *Trends Neurosci.* **27,** 329–336
5. Sine, S. M., and Engel, A. G. (2006) *Nature* **440,** 448–455
6. Unwin, N., Miyazawa, A., Li, J., and Fujiyoshi, Y. (2002) *J. Mol. Biol.* **319,** 1165–1176
7. Unwin, N. (2003) *FEBS Lett.* **555,** 91–95
8. Bourne, Y., Talley, T. T., Hansen, S. B., Taylor, P., and Marchot, P. (2005) *EMBO J.* **24,** 1512–1522
9. Celie, P. H., Kasheverov, I. E., Mordvintsev, D. Y., Hogg, R. C., van Nierop, P., van Elk, R., van Rossum-Fikkert, S. E., Zhmak, M. N., Bertrand, D.,

Tsetlin, V., Sixma, T. K., and Smit, A. B. (2005) *Nat. Struct. Mol. Biol.* **12,** 582–588
10. Gao, F., Bren, N., Burghardt, T. P., Hansen, S., Henchman, R. H., Taylor, P., McCammon, J. A., and Sine, S. M. (2005) *J. Biol. Chem.* **280,** 8443–8451
11. Hansen, S. B., Sulzenbacher, G., Huxford, T., Marchot, P., Taylor, P., and Bourne, Y. (2005) *EMBO J.* **24,** 3635–3646
12. Mukhtasimova, N., Free, C., and Sine, S. M. (2005) *J. Gen. Physiol.* **126,** 23–39
13. Venkatachalan, S. P., and Czajkowski, C. (2008) *Proc. Natl. Acad. Sci. U. S. A.* **105,** 13604–13609
14. Cheng, X., Lu, B., Grant, B., Law, R. J., and McCammon, J. A. (2006) *J. Mol. Biol.* **355,** 310–324
15. Cheng, X., Wang, H., Grant, B., Sine, S. M., and McCammon, J. A. (2006) *PLoS Comput. Biol.* **2,** e134
16. Law, R. J., Henchman, R. H., and McCammon, J. A. (2005) *Proc. Natl. Acad. Sci. U. S. A.* **102,** 6813–6818
17. Liu, X., Xu, Y., Li, H., Wang, X., Jiang, H., and Barrantes, F. J. (2008) *PLoS Comput. Biol.* **4,** e19
18. Taly, A., Corringer, P. J., Grutter, T., Prado de Carvalho, L., Karplus, M., and Changeux, J. P. (2006) *Proc. Natl. Acad. Sci. U. S. A.* **103,** 16965–16970
19. Khatri, A., Sedelnikova, A., and Weiss, D. S. (2009) *Biophys. J.* **96,** 45–55
20. Thompson, A. J., Padgett, C. L., and Lummis, S. C. (2006) *J. Biol. Chem.* **281,** 16576–16582
21. Zhang, J., Xue, F., and Chang, Y. (2009) *J. Physiol.* **587,** 139–153
22. Bocquet, N., Nury, H., Baaden, M., Le Poupon, C., Changeux, J. P., Delarue, M., and Corringer, P. J. (2009) *Nature* **457,** 111–114
23. Hilf, R. J., and Dutzler, R. (2009) *Nature* **457,** 115–118
24. Young, A. B., and Snyder, S. H. (1973) *Proc. Natl. Acad. Sci. U. S. A.* **70,** 2832–2836
25. Young, A. B., and Snyder, S. H. (1974) *Proc. Natl. Acad. Sci. U. S. A.* **71,** 4002–4005
26. Pless, S. A., and Lynch, J. W. (2008) *Clin. Exp. Pharmacol. Physiol.* **35,** 1137–1142
27. Chang, Y., and Weiss, D. S. (2002) *Nat. Neurosci.* **5,** 1163–1168
28. Dahan, D. S., Dibas, M. I., Petersson, E. J., Auyeung, V. C., Chanda, B., Bezanilla, F., Dougherty, D. A., and Lester, H. A. (2004) *Proc. Natl. Acad. Sci. U. S. A.* **101,** 10195–10200
29. Mourot, A., Bamberg, E., and Rettinger, J. (2008) *J. Neurochem.* **105,** 413–424
30. Muroi, Y., Czajkowski, C., and Jackson, M. B. (2006) *Biochemistry* **45,** 7013–7022
31. Pless, S. A., Dibas, M. I., Lester, H. A., and Lynch, J. W. (2007) *J. Biol. Chem.* **282,** 36057–36067
32. Muroi, Y., Theusch, C. M., Czajkowski, C., and Jackson, M. B. (2009) *Biophys. J.* **96,** 499–509
33. Pless, S. A., and Lynch, J. W. (2009) *J. Neurochem.* **108,** 1585–1594
34. Virkki, L. V., Murer, H., and Forster, I. C. (2006) *J. Biol. Chem.* **281,** 28837–28849
35. Wagner, D. A., and Czajkowski, C. (2001) *J. Neurosci.* **21,** 67–74
36. Grudzinska, J., Schemm, R., Haeger, S., Nicke, A., Schmalzing, G., Betz, H., and Laube, B. (2005) *Neuron* **45,** 727–739
37. Pless, S. A., Millen, K. S., Hanek, A. P., Lynch, J. W., Lester, H. A., Lummis, S. C., and Dougherty, D. A. (2008) *J. Neurosci.* **28,** 10937–10942
38. Kash, T. L., Trudell, J. R., and Harrison, N. L. (2004) *Biochem. Soc. Trans.* **32,** 540–546
39. Newell, J. G., and Czajkowski, C. (2003) *J. Biol. Chem.* **278,** 13166–13172
40. Padgett, C. L., and Lummis, S. C. (2008) *J. Biol. Chem.* **283,** 2702–2708
41. Unwin, N. (2005) *J. Mol. Biol.* **346,** 967–989
42. Celie, P. H., van Rossum-Fikkert, S. E., van Dijk, W. J., Brejc, K., Smit, A. B., and Sixma, T. K. (2004) *Neuron* **41,** 907–914
43. Lee, W. Y., and Sine, S. M. (2005) *Nature* **438,** 243–247
44. Rajendra, S., Vandenberg, R. J., Pierce, K. D., Cunningham, A. M., French, P. W., Barry, P. H., and Schofield, P. R. (1995) *EMBO J.* **14,** 2987–2998
45. Vandenberg, R. J., Handford, C. A., and Schofield, P. R. (1992) *Neuron* **9,** 491–496
46. Absalom, N. L., Lewis, T. M., Kaplan, W., Pierce, K. D., and Schofield, P. R. (2003) *J. Biol. Chem.* **278,** 50151–50157
47. Beato, M., Groot-Kormelink, P. J., Colquhoun, D., and Sivilotti, L. G. (2002) *J. Gen. Physiol.* **119,** 443–466
48. Lewis, T. M., Schofield, P. R., and McClellan, A. M. (2003) *J. Physiol.* **549,** 361–374
49. Deleted in proof
50. Mukhtasimova, N., and Sine, S. M. (2007) *J. Neurosci.* **27,** 4110–4119
51. Purohit, P., and Auerbach, A. (2007) *J. Gen. Physiol.* **130,** 569–579
52. Kash, T. L., Jenkins, A., Kelley, J. C., Trudell, J. R., and Harrison, N. L. (2003) *Nature* **421,** 272–275
53. Kash, T. L., Kim, T., Trudell, J. R., and Harrison, N. L. (2004) *Neurosci. Lett.* **371,** 230–234
54. Sala, F., Mulet, J., Sala, S., Gerber, S., and Criado, M. (2005) *J. Biol. Chem.* **280,** 6642–6647
55. Xiu, X., Hanek, A. P., Wang, J., Lester, H. A., and Dougherty, D. A. (2005) *J. Biol. Chem.* **280,** 41655–41666
56. Kash, T. L., Dizon, M. J., Trudell, J. R., and Harrison, N. L. (2004) *J. Biol. Chem.* **279,** 4887–4893

Ligand-specific Conformational Changes in the α1 Glycine Receptor Ligand-binding Domain

Stephan A. Pless and Joseph W. Lynch

J. Biol. Chem. 2009, 284:15847-15856.
doi: 10.1074/jbc.M809343200 originally published online March 13, 2009
